Performance bounds for modal analysis using sparse linear arrays

Yuanxin Li[a], Ali Pezeshki[b], Louis L. Scharf[c], and Yuejie Chi[a]

[a]Department of Electrical and Computer Engineering, The Ohio State University
[b]Department of Electrical and Computer Engineering, Colorado State University
[c]Department of Mathematics, Colorado State University

ABSTRACT

We study the performance of modal analysis using sparse linear arrays (SLAs) such as nested and co-prime arrays, in both first-order and second-order measurement models. We treat SLAs as constructed from a subset of sensors in a dense uniform linear array (ULA), and characterize the performance loss of SLAs with respect to the ULA due to using much fewer sensors. In particular, we claim that, provided the same aperture, in order to achieve comparable performance in terms of Cramér-Rao bound (CRB) for modal analysis, SLAs require more snapshots, of which the number is about the number of snapshots used by ULA times the compression ratio in the number of sensors. This is shown analytically for the case with one undamped mode, as well as empirically via extensive numerical experiments for more complex scenarios. Moreover, the misspecified CRB proposed by Richmond and Horowitz is also studied, where SLAs suffer more performance loss than their ULA counterpart.

Keywords: sparse linear array, Cramér-Rao bound, compression ratio, misspecification

1. INTRODUCTION

Sparse linear arrays (SLAs), such as minimum redundancy arrays,[1] nested arrays[2] and co-prime arrays,[3] have attracted a great deal of attention in recent times, especially for beamforming and direction finding. Leveraging second-order statistics as well as the geometry of difference co-arrays, these non-uniform array geometries are capable of identifying (in the absence of noise) more modes than the number of sensors[2–4] due to the increased degrees of freedom. Even without going into the co-array domain, they exhibit lower Cramér-Rao bounds (CRBs) and higher resolvability[5,6] when their measurements are directly exploited, compared with a uniform linear array (ULA) that is composed of the same number of sensors. These SLAs, investigated in Ref. 5, 6, have the same number of sensors with the ULA, but they can benefit from the significantly increased size of aperture because of well-designed geometries.

In this paper, inspired by Ref. 7, we consider SLAs as sub-arrays constructed by a subset of sensors in a dense ULA with the same aperture of the SLAs. Thus, different from Ref. 5, 6, the SLAs studied in this paper have the same aperture with the ULA, but consist of much fewer sensors. This viewpoint is taken in order to characterize the *performance degeneration* of SLAs with respect to the original ULA, due to using fewer sensors. Rather than examining performance of specific algorithms, we adopt CRB as the performance metric for modal analysis, since the celebrated CRB provides a lower bound on the variances of unbiased mode estimates. Various CRB expressions of SLAs have been presented under both first-order and second-order assumptions of the measurement model.[8–12]

Our intuition is that, provided the same aperture, in order to achieve comparable performance in terms of CRB for modal analysis, SLAs require a larger number of snapshots than the ULA. The number of snapshots required is about the number of snapshots used by the ULA times the compression ratio in the number of sensors. This is consistent with observations made in other recent studies (e.g., Ref. 7, 13) that compare the performance of SLAs with that of a ULA of similar aperture. We verify this intuitive result analytically in the case where there is only one undamped mode in the first-order measurement model.

Emails: li.3822@osu.edu, {Ali.Pezeshki, Louis.Scharf}@colostate.edu, chi.97@osu.edu

Given a fixed number of sensors, we analytically show that the optimal SLA geometry from the perspective of Fisher information is to build the SLA as two sub-arrays of consecutive elements taken from the two ends of the ULA. Then we show that under the same number of snapshots and per-sensor signal-to-noise ratio (SNR), the ratio of the CRB of the optimal SLA to that of the ULA is in the order of compression ratio in the number of sensors. As a consequence, assuming the ratio of per-sensor SNRs, determined by the average energy of mode amplitudes, keeps almost as a constant while increasing the number of snapshots, the CRB loss of SLAs can be compensated by more snapshots. This claim is also empirically verified via extensive numerical experiments for more complex scenarios, even with damped modes, in both first-order and second-order measurement models.

In addition, we conduct numerical experiments to compare the behaviors of SLAs under model misspecification via the misspecified CRB (MCRB), recently proposed in Ref. 14, where the sensors are not perfectly located at integer multiples of half wavelength. We demonstrate that SLAs not only yield a higher MCRB than ULA in estimating an undamped mode, but also bear wider MCRB confidence intervals.

The remainder of the paper is organized as follows. First, we give the formulations of both first-order and second-order measurement models, and discuss the corresponding CRB expressions in Sec. 2. In Sec. 3, given a fixed number of sensors, we derive the optimal SLA geometry for estimating a single undamped mode, and the ratio of its CRB to that of the ULA. Then we provide extensive numerical experiments in Sec. 4 to validate the CRB compensation by using more snapshots in more complex scenarios. Next, we examine misspecified CRB in Sec. 5. Finally, in Sec. 6 we conclude and discuss the future work.

2. MODEL FORMULATION AND CRB

Consider a linear array composed of m_s sensors, whose locations are specified by $\mathbb{I}_s = \{i_0, i_1, \ldots, i_{m_s-1}\}$ in units of half wavelength ($\lambda/2$) in space. Suppose there are p potentially damped modes, represented as $z_k = \rho_k e^{j2\pi f_k}$, with $\rho_k \in \mathbb{R}^+$ and $f_k \in [0, 1)$, $k = 1, 2, \ldots, p$. Then the nth measurement snapshot observed by the linear array can be formulated as a linear combination of p weighted steering vectors, perhaps corrupted by additive noise, as

$$\boldsymbol{y}[n] = \boldsymbol{V}(\boldsymbol{z}, \mathbb{I}_s)\, \boldsymbol{x}[n] + \boldsymbol{e}[n], \quad n = 0, 1, \ldots, N-1, \tag{1}$$

where $\boldsymbol{y}[n] = [y_0[n], y_1[n], \ldots, y_{m_s-1}[n]]^T \in \mathbb{C}^{m_s}$ is the nth array measurement snapshot, $\boldsymbol{x}[n] = [x_1[n], x_2[n], \ldots, x_p[n]]^T \in \mathbb{C}^p$ is the nth mode amplitude vector, and $\boldsymbol{e}[n] = [e_0[n], e_1[n], \ldots, e_{m_s-1}[n]]^T \in \mathbb{C}^{m_s}$ is the additive noise vector. Moreover, $\boldsymbol{V}(\boldsymbol{z}, \mathbb{I}_s) \in \mathbb{C}^{m_s \times p}$, of which each column is the steering vector corresponding to one mode, is a generalized Vandermode matrix, expressed as

$$\boldsymbol{V}(\boldsymbol{z}, \mathbb{I}_s) = [\boldsymbol{v}(z_1, \mathbb{I}_s), \boldsymbol{v}(z_2, \mathbb{I}_s), \ldots, \boldsymbol{v}(z_p, \mathbb{I}_s)], \tag{2}$$

where $\boldsymbol{v}(z_k, \mathbb{I}_s) = \left[z_k^{i_0}, z_k^{i_1}, \ldots, z_k^{i_{m_s-1}}\right]^T$, $k = 1, 2, \ldots, p$.

Below we discuss the first-order and second-order measurement model, respectively, and the corresponding CRB expressions.

2.1 First-Order Measurement Model

Here, the mode amplitude vectors $\boldsymbol{x}[n]$, $n = 0, 1, \ldots, N-1$, are assumed unknown but deterministic, while the noise vectors $\boldsymbol{e}[n]$, $n = 0, 1, \ldots, N-1$, are i.i.d. generated from Gaussian distribution as

$$\boldsymbol{e}[n] \sim \mathcal{CN}\left(\boldsymbol{0}, \sigma_e^2 \boldsymbol{I}\right). \tag{3}$$

In this case, the CRB matrix of estimating the mode parameters $\boldsymbol{z}$ can be written as[7]

$$\mathbf{CRB}_f(\boldsymbol{z}, \mathbb{I}_s) = \sigma_e^2 \left[\left(\boldsymbol{D}^H(\boldsymbol{z}, \mathbb{I}_s)\left[\boldsymbol{I} - \boldsymbol{P}_{\boldsymbol{V}(\boldsymbol{z}, \mathbb{I}_s)}\right]\boldsymbol{D}(\boldsymbol{z}, \mathbb{I}_s)\right) \odot \left(\sum_{n=0}^{N-1} \boldsymbol{x}[n]\, \boldsymbol{x}^H[n]\right)^T\right]^{-1}, \tag{4}$$

where $\odot$ denotes Hadamard product, $\boldsymbol{P}_{\boldsymbol{V}(\boldsymbol{z},\mathbb{I}_s)}$ is the orthogonal projection onto the column spans of $\boldsymbol{V}(\boldsymbol{z},\mathbb{I}_s)$, and $\boldsymbol{D}(\boldsymbol{z},\mathbb{I}_s)$ is defined as $\boldsymbol{D}(\boldsymbol{z},\mathbb{I}_s) = \left[\frac{\partial \boldsymbol{v}(z_1,\mathbb{I}_s)}{\partial z_1}, \frac{\partial \boldsymbol{v}(z_2,\mathbb{I}_s)}{\partial z_2}, \ldots, \frac{\partial \boldsymbol{v}(z_p,\mathbb{I}_s)}{\partial z_p}\right]$. Further, define the sample covariance matrix $\boldsymbol{\Sigma}_s = \frac{1}{N}\sum_{n=0}^{N-1} \boldsymbol{x}[n]\boldsymbol{x}^H[n]$, then the CRB matrix can be rewritten as

$$\mathbf{CRB}_f(\boldsymbol{z},\mathbb{I}_s) = \frac{\sigma_e^2}{N}\left[\left(\boldsymbol{D}^H(\boldsymbol{z},\mathbb{I}_s)\left[\boldsymbol{I}-\boldsymbol{P}_{\boldsymbol{V}(\boldsymbol{z},\mathbb{I}_s)}\right]\boldsymbol{D}(\boldsymbol{z},\mathbb{I}_s)\right)\odot\boldsymbol{\Sigma}_s^T\right]^{-1}. \tag{5}$$

The CRB expression in Eq. (4) is valid when the number of sensors m_s is larger than the number of modes p, otherwise the CRB becomes unbounded due to singularity of the Fisher information matrix.

2.2 Second-Order Measurement Model

Here, the mode amplitude vectors $\boldsymbol{x}[n]$, $n = 0, 1, \ldots, N-1$, and the noise vectors $\boldsymbol{e}[n]$, $n = 0, 1, \ldots, N-1$, are assumed uncorrelated and i.i.d. drawn from proper Gaussian distributions

$$\boldsymbol{x}[n] \sim \mathcal{CN}(\boldsymbol{0},\boldsymbol{\Sigma}) \quad \text{and} \quad \boldsymbol{e}[n] \sim \mathcal{CN}\left(\boldsymbol{0},\sigma_e^2\boldsymbol{I}\right), \tag{6}$$

respectively.

Suppose the unknown variables are denoted by $\boldsymbol{\alpha} = [\alpha_1, \alpha_2, \ldots, \alpha_K]$, containing both mode parameters and other nuisance parameters. Let $\boldsymbol{R} = \boldsymbol{V}(\boldsymbol{z},\mathbb{I}_s)\boldsymbol{\Sigma}\boldsymbol{V}^H(\boldsymbol{z},\mathbb{I}_s) + \sigma_e^2\boldsymbol{I}$, and let $\boldsymbol{r}$ be the vectorization of $\boldsymbol{R}$ as $\boldsymbol{r} = \mathrm{vec}(\boldsymbol{R})$. Also denote the derivative of $\boldsymbol{r}$ with respect to $\boldsymbol{\alpha}$ by $\frac{\partial \boldsymbol{r}}{\partial \boldsymbol{\alpha}} = \left[\frac{\partial \boldsymbol{r}}{\partial \alpha_1}, \frac{\partial \boldsymbol{r}}{\partial \alpha_2}, \ldots, \frac{\partial \boldsymbol{r}}{\partial \alpha_K}\right]$. Then the CRB matrix for the estimation of all the unknown parameters, denoted by $\mathbf{CRB}_s(\boldsymbol{\alpha},\mathbb{I}_s)$, becomes[10,15]

$$\mathbf{CRB}_s(\boldsymbol{\alpha},\mathbb{I}_s) = \frac{1}{N}\left[\left(\frac{\partial \boldsymbol{r}}{\partial \boldsymbol{\alpha}}\right)^H\left(\boldsymbol{R}^T\otimes\boldsymbol{R}\right)^{-1}\frac{\partial \boldsymbol{r}}{\partial \boldsymbol{\alpha}}\right]^{-1}, \tag{7}$$

where $\otimes$ denotes the Kronecker product. Unlike the first-order expression in Eq. (4), this expression is valid even when the number of modes p is greater than the number of sensors m_s.

2.3 Discussions

When assuming $\boldsymbol{x}[n]$'s are i.i.d. generated from the proper Gaussian distribution $\mathcal{CN}(\boldsymbol{0},\boldsymbol{\Sigma})$, $\boldsymbol{\Sigma}_s$ is the sample covariance matrix, which will converge to the real covariance matrix $\boldsymbol{\Sigma}$ with N approaching infinity. Nevertheless, replacing the sample covariance matrix in Eq. (4) with the covariance matrix does not yield Eq. (7). Furthermore, with finite N, different realizations of $\boldsymbol{x}[n]$'s will lead to different CRB matrices $\mathbf{CRB}_f(\boldsymbol{z},\mathbb{I}_s)$ in the first-order measurement model. Therefore, when the number of modes is small, the ensemble of $\mathbf{CRB}_f(\boldsymbol{z},\mathbb{I}_s)$ is more revealing and indicative of performance than the CRB matrix $\mathbf{CRB}_s(\boldsymbol{\alpha},\mathbb{I}_s)$ obtained in the second-order measurement model, which is determined by the population covariance matrix $\boldsymbol{\Sigma}$. In this paper, we focus on the CRB matrices in the first-order measurement model, while few numerical experiments are conducted in the second-order measurement model.

3. THEORETICAL ANALYSIS WITH ONE UNDAMPED MODE

In the first-order measurement model, consider a scenario where only one undamped mode z_1 exists, i.e. $z_1 = e^{j2\pi f_1}$, so $|z_1| = 1$. Suppose a linear array is composed of m_s sensors, specified as $\mathbb{I}_s = \{i_0, i_1, \ldots, i_{m_s-1}\}$, then the CRB of estimating the mode parameter z_1 can be simplified as

$$\mathrm{CRB}_f(z_1,\mathbb{I}_s) = \left[\frac{\sum_{n=0}^{N-1}|x_1[n]|^2}{\sigma_e^2}\cdot\left(\sum_{k=0}^{m_s-1} i_k^2 - \frac{\left(\sum_{k=0}^{m_s-1} i_k\right)^2}{m_s}\right)\right]^{-1} = \frac{1}{N\cdot\mathrm{SNR}_f(z_1,\mathbb{I}_s)\cdot J_f(z_1,\mathbb{I}_s)}, \tag{8}$$

where

$$\mathrm{SNR}_f(z_1,\mathbb{I}_s) = \frac{\sum_{n=0}^{N-1}|x_1[n]|^2}{N\sigma_e^2} \tag{9}$$

represents the per-sensor SNR. Besides, $J_f(z_1, \mathbb{I}_s)$ is defined as

$$J_f(z_1, \mathbb{I}_s) = \sum_{k=0}^{m_s-1} i_k^2 - \frac{\left(\sum_{k=0}^{m_s-1} i_k\right)^2}{m_s} = \frac{1}{m_s} \sum_{k=0}^{m_s-1} \sum_{t=k}^{m_s-1} (i_k - i_t)^2, \tag{10}$$

which is determined by the sum of squared distances between sensors.

3.1 Optimal Array Configuration with Given Aperture

It is somewhat indicated by Eq. (10) that increasing the aperture of a linear array will introduce a larger $J_f(z_1, \mathbb{I}_s)$, thereby resulting in a lower $\mathrm{CRB}_f(z_1, \mathbb{I}_s)$. However, a more interesting question concerns the optimal array configuration to maximize $J_f(z_1, \mathbb{I}_s)$ for a given aperture.

Fixing the number of sensors, we have the following result about the optimal SLA configuration to maximize $J_f(z_1, \mathbb{I}_s)$, which is proved in App. A.

Theorem 1. *Suppose $\mathbb{I}_{ula}$ is an m-sensor ULA, specified as $\mathbb{I}_{ula} = \{0, 1, \ldots, m-1\}$. Assume m_s is an even integer, where $2 \le m_s \le m$, and let $\mathbb{I}_s$ denote an m_s-sensor linear array, which is constructed by a subset of sensors in $\mathbb{I}_{ula}$ such that $\mathbb{I}_s = \{i_0, i_1, \ldots, i_{m_s-1}\} \subseteq \mathbb{I}_{ula}$. Consequently, the aperture of $\mathbb{I}_s$ is restricted by $m-1$, and the maximum of $J_f(z_1, \mathbb{I}_s)$ is achieved by consecutively picking half of the sensors from each end of ULA. Specifically, from the perspective of Fisher information, the optimal m_s-sensor linear array will be $\mathbb{I}_{s-optimal} = \{0, 1, \ldots, m_s/2-1\} \cup \{m - m_s/2, m - m_s/2 + 1, \ldots, m-1\}$.*

Remark 1. *When m_s is an odd integer, where $3 \le m_s \le m$, the optimal m_s-sensor linear array will be $\mathbb{I}_{s-optimal} = \{0, 1, \ldots, (m_s-1)/2\} \cup \{m - (m_s-1)/2, m - (m_s-3)/2, \ldots, m-1\}$ or $\mathbb{I}_{s-optimal} = \{0, 1, \ldots, (m_s-3)/2\} \cup \{m - (m_s+1)/2, m - (m_s-1)/2, \ldots, m-1\}$.*

Remark 2. *For an even m and an even m_s, it is not difficult to show that $\mathbb{I}_{s-worst} = \{0, m-1\} \cup \{m/2 - m_s/2 + 1, m/2 - m_s/2 + 2, \ldots, m/2 + m_s/2 - 2\}$ will yield the smallest $J_f(z_1, \mathbb{I}_s)$ among all the m_s-sensor linear arrays with a fixed aperture $m-1$.*

Remark 3. *Note that this optimal array geometry is derived when there is a single undamped mode, and therefore is not guaranteed to be optimal when more modes are present.*

3.2 CRB Ratios

We now characterize the performance loss of SLAs in one undamped mode scenario with respect to the dense ULA, due to making use of much fewer sensors. Define η as the ratio of the number of sensors of the ULA to that of the SLAs as $\eta = m/m_s$, referred to as the compression ratio in the number of sensors, thus $\eta \ge 1$. The following results connect the performance loss of SLAs in terms of CRB with the compression ratio η.

Theorem 2. *Suppose $\mathbb{I}_{ula}$ is an m-sensor ULA, specified as $\mathbb{I}_{ula} = \{0, 1, \ldots, m-1\}$. Assume m_s is an even integer, where $2 \le m_s \le m$, and let $\mathbb{I}_s$ denote an m_s-sensor linear array, which is constructed by a subset of sensors in $\mathbb{I}_{ula}$ such that $\mathbb{I}_s = \{i_0, i_1, \ldots, i_{m_s-1}\} \subseteq \mathbb{I}_{ula}$. Then we have*

$$\frac{J_f(z_1, \mathbb{I}_{ula})}{J_f(z_1, \mathbb{I}_s)} \ge \frac{J_f(z_1, \mathbb{I}_{ula})}{J_f(z_1, \mathbb{I}_{s-optimal})} \ge \frac{1}{3}\eta,$$

where $\mathbb{I}_{s-optimal} = \{0, 1, \ldots, m_s/2-1\} \cup \{m - m_s/2, m - m_s/2 + 1, \ldots, m-1\}$. Further, we have

$$\frac{\mathrm{CRB}_f(z_1, \mathbb{I}_s)}{\mathrm{CRB}_f(z_1, \mathbb{I}_{ula})} = \frac{N_{ula} \cdot \mathrm{SNR}_f(z_1, \mathbb{I}_{ula}) \cdot J_f(z_1, \mathbb{I}_{ula})}{N_s \cdot \mathrm{SNR}_f(z_1, \mathbb{I}_s) \cdot J_f(z_1, \mathbb{I}_s)} \ge \frac{1}{3}\eta \cdot \frac{N_{ula}}{N_s} \cdot \frac{\mathrm{SNR}_f(z_1, \mathbb{I}_{ula})}{\mathrm{SNR}_f(z_1, \mathbb{I}_s)}.$$

Remark 4. *When m_s is an odd integer satisfying $3 \le m_s \le m$, we can obtain the same bound that is $J_f(z_1, \mathbb{I}_{ula}) / J_f(z_1, \mathbb{I}_s) \ge \eta/3$.*

Remark 5. *Specifically, consider a co-prime array specified as $\mathbb{I}_{coprime} = \{0, m_2, 2m_2, \ldots, (m_1-1)m_2\} \cup \{m_1, 2m_1, \ldots, (2m_2-1)m_1\}$, where the greatest common factor $(m_1, m_2) = 1$ and $m_1 > m_2$. Hence, this co-prime array totally contains $m_{coprime} = m_1 + 2m_2 - 1$ sensors, and has an aperture as $A_{coprime} = (2m_2 - 1)\, m_1$.*

We would like to compare this co-prime array with a ULA, which has an aperture as $A_{ula} = (2m_2 - 1)\, m_1$ *as well, so we consider a ULA specified as* $\mathbb{I}_{ula} = \{0, 1, \ldots, (2m_2 - 1)\, m_1\}$*, which is composed of* $m_{ula} = (2m_2 - 1)\, m_1 + 1$ *sensors. Assuming* $m_2 \geq 5$*, we have*

$$\frac{J_f\left(z_1, \mathbb{I}_{ula}\right)}{J_f\left(z_1, \mathbb{I}_{coprime}\right)} > 0.88 \cdot \frac{m_{ula}}{m_{coprime}}.$$

The proof of Thm. 2 is provided in App. B. In this one undamped mode scenario, the per-sensor SNR happens to be independent on the array geometry. So provided with same mode amplitudes, we obtain $\mathrm{SNR}_f\left(z_1, \mathbb{I}_{ula}\right) = \mathrm{SNR}_f\left(z_1, \mathbb{I}_s\right)$, and further $\mathrm{CRB}_f\left(z_1, \mathbb{I}_s\right) / \mathrm{CRB}_f\left(z_1, \mathbb{I}_{ula}\right) \geq \eta/3$, which implies that compared with the ULA, an m_s-sensor SLA suffers a CRB loss in the order of compression ratio η.

If the per-sensor SNR can perform almost as a constant while increasing the number of snapshots, we know

$$\frac{\mathrm{CRB}_f\left(z_1, \mathbb{I}_s\right)}{\mathrm{CRB}_f\left(z_1, \mathbb{I}_{ula}\right)} \approx c\eta \frac{N_{ula}}{N_s}, \tag{11}$$

for some constant c. In such a case, to achieve comparable performance in terms of CRB for modal analysis, the number of snapshots required by SLAs needs to be about the number of snapshots used by ULA times the compression ratio in the number of sensors, up to some constant. Actually, in practice, it is quite common to approximate the per-sensor SNR, determined by the average energy of mode amplitudes, by a constant with respect to the number of snapshots. This can be satisfied, for example, in the case where the mode amplitudes are i.i.d. generated from some complex Gaussian distribution. As long as the number of snapshots is large enough, based on the law of large numbers, the sample variance will concentrate around the population variance, which guarantees an almost constant per-sensor SNR despite the change of number of snapshots.

Before concluding this section, we consider the asymptotic behaviors of CRB comparisons by assuming both $m \to \infty$ and $m_s \to \infty$ while keeping η fixed. Supposing both m and m_s are even integers, where $2 \leq m_s \leq m$, besides $\mathbb{I}_{ula}$ and $\mathbb{I}_{s-optimal}$, we also examine the following array configurations:

$$\begin{aligned}
&\mathbb{I}_{ula-short} = \{0, 1, \ldots, m_s - 1\}; \\
&\mathbb{I}_{s-worst} = \{0, m-1\} \cup \{m/2 - m_s/2 + 1, m/2 - m_s/2 + 2, \ldots, m/2 + m_2/2 - 2\}.
\end{aligned}$$

Accordingly, $\mathbb{I}_{ula}$ has the same aperture with $\mathbb{I}_{s-optimal}$ and $\mathbb{I}_{s-worst}$, but contains more sensors, while $\mathbb{I}_{ula-short}$ is constructed by the same number of sensors with $\mathbb{I}_{s-optimal}$ and $\mathbb{I}_{s-worst}$, but possesses a much smaller aperture. Then we have

$$\frac{J_f\left(z_1, \mathbb{I}_{ula}\right)}{J_f\left(z_1, \mathbb{I}_{ula-short}\right)} = \frac{m\left(m^2 - 1\right)/12}{m_s\left(m_s^2 - 1\right)/12} \overset{m\to\infty, m_s\to\infty}{=} \eta^3; \tag{12}$$

$$\frac{J_f\left(z_1, \mathbb{I}_{ula}\right)}{J_f\left(z_1, \mathbb{I}_{s-optimal}\right)} = \frac{m\left(m^2 - 1\right)/12}{m_s\left(m_s^2 - 3mm_s + 3m^2 - 1\right)/12} \overset{m\to\infty, m_s\to\infty}{=} \eta \cdot \frac{\eta^2}{3\eta^2 - 3\eta + 1} \in \left[\frac{1}{3}\eta, \eta\right]; \tag{13}$$

$$\frac{J_f\left(z_1, \mathbb{I}_{s-optimal}\right)}{J_f\left(z_1, \mathbb{I}_{ula-short}\right)} = \frac{m_s\left(m_s^2 - 3mm_s + 3m^2 - 1\right)/12}{m_s\left(m_s^2 - 1\right)/12} \overset{m\to\infty, m_s\to\infty}{=} 1 + 3\eta(\eta - 1); \tag{14}$$

and

$$\frac{J_f\left(z_1, \mathbb{I}_{s-worst}\right)}{J_f\left(z_1, \mathbb{I}_{ula-short}\right)} = \frac{\left(m_s^3 - 6m_s^2 + 11m_s + 6m^2 - 12m\right)/12}{m_s\left(m_s^2 - 1\right)/12} \overset{m\to\infty, m_s\to\infty}{=} 1. \tag{15}$$

With the same number of snapshots and per-sensor SNR, the ratio of CRBs between the two ULAs, i.e. $J_f\left(z_1, \mathbb{I}_{ula}\right) / J_f\left(z_1, \mathbb{I}_{ula-short}\right)$, is roughly in the order of $\mathcal{O}\left(\eta^3\right)$, determined by the third order of the compression ratio in the number of sensors. Then for an m_s-sensor linear array, the smallest CRB is achieved by $\mathbb{I}_{s-optimal}$, which has the same aperture as $\mathbb{I}_{ula}$ as $m-1$ and only loses a factor η with respect to $\mathbb{I}_{ula}$. In addition, for some m_s-sensor array, like $\mathbb{I}_{s-worst}$, even with aperture $m-1$, it can only achieve comparable CRB performance as $\mathbb{I}_{ula-short}$.

4. NUMERICAL CRB COMPARISONS

In previous section, we have analytically argued that provided the same aperture, for one undamped mode scenario in the first-order measurement model, the CRB loss of SLAs resulting from lack of sensors with respect to ULA can be compensated by more measurement snapshots, roughly in the number of snapshots used by ULA times the compression ratio in the number of sensors. This section works as a supplementary part to support this argument via providing extensive numerical experiments in more complex scenarios in both first-order and second-order measurement models.

Consider the following array configurations:

$$\begin{aligned}
&\mathbb{I}_{mra} = \{0,1,4,10,16,22,28,30,33,35\},\ m_{mra} = 10,\ A_{mra} = 35;\\
&\mathbb{I}_{nested} = \{1,2,3\} \cup \{4,8,12,16,20,24,28,32,36\},\ m_{nested} = 12,\ A_{nested} = 35;\\
&\mathbb{I}_{coprime} = \{0,3,6,9,12,15,18\} \cup \{7,14,21,28,35\},\ m_{coprime} = 12,\ A_{coprime} = 35;\\
&\mathbb{I}_{ula} = \{0,1,2,3,4,5,\ldots,35\},\ m_{ula} = 36,\ A_{ula} = 35;\\
&\mathbb{I}_{ula-short} = \{0,1,2,3,4,5,6,7,8,9,10,11\},\ m_{ula-short} = 12,\ A_{ula-short} = 11;\\
&\mathbb{I}_{stretched} = \{0,1,2,3,4,5\} \cup \{30,31,32,33,34,35\},\ m_{stretched} = 12,\ A_{stretched} = 35,
\end{aligned}$$

where except for $\mathbb{I}_{ula-short}$, all the other linear arrays have the same aperture.

4.1 CRB Comparisons in First-Order Measurement Model

Two modes are specified as $\boldsymbol{z} = [z_1, z_2]^T = [e^{j2\pi f_1}, 0.95 \cdot e^{j2\pi f_2}]^T$, with $f_1 = 0.14$ and $f_2 = 0.71$. Assume the mode amplitude vectors are i.i.d. drawn from $\mathcal{CN}[\mathbf{0}, \boldsymbol{\Sigma}]$, where $\boldsymbol{\Sigma} = \begin{bmatrix} 1 & \rho \\ \rho & 1 \end{bmatrix}$ with $\rho = 0.8$. The per-sensor SNR is defined as

$$\mathrm{SNR}_f(\boldsymbol{z}, \mathbb{I}) = 10\log_{10} \frac{\sum_{n=0}^{N-1} \|\boldsymbol{V}(\boldsymbol{z}, \mathbb{I})\, \boldsymbol{x}[n]\|_2^2}{Nm\sigma_e^2}. \tag{16}$$

The number of snapshots for all arrays is set as $N = 200$. Then the CRBs of estimating the two modes by different arrays with respect to per-sensor SNR are shown in Fig. 1. Figure 1 indicates that the 36-sensor ULA

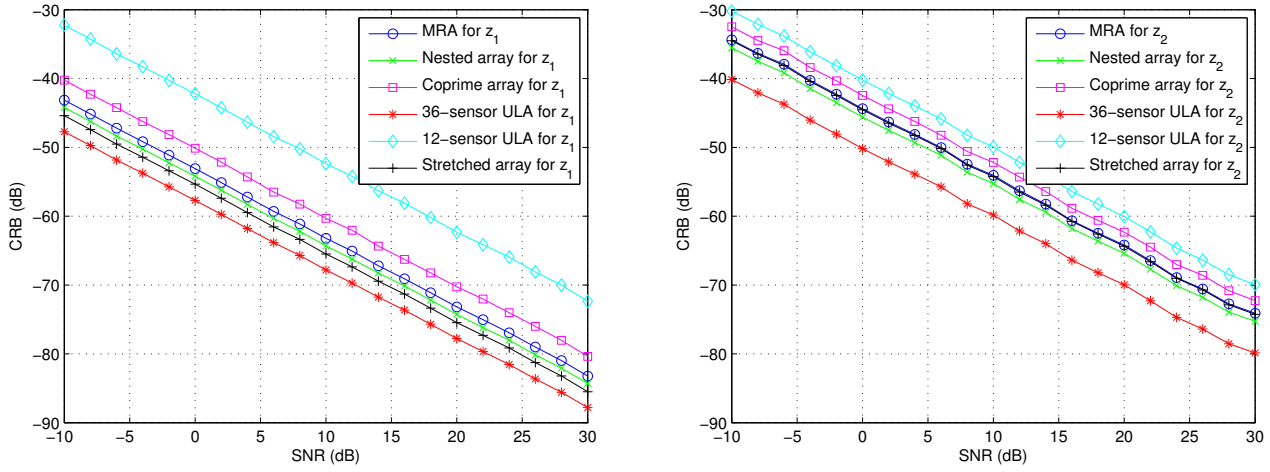

(a) CRBs for z_1 (b) CRBs for z_2

Figure 1. CRB comparisons with respect to per-sensor SNR, when the number of snapshots for all arrays set as $N = 200$ in the first-order measurement model.

$\mathbb{I}_{ula}$ has the smallest CRBs, while the 12-sensor ULA $\mathbb{I}_{ula-short}$ has the largest CRBs, which accords with one undamped mode case. However, one array may have a different performance when dealing with a damped mode from that of an undamped mode. In general, estimating a damped mode will suffer from a larger CRB.

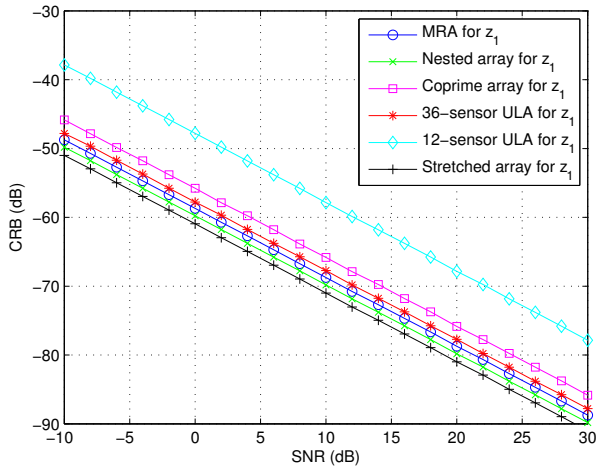

(a) CRBs for z_1

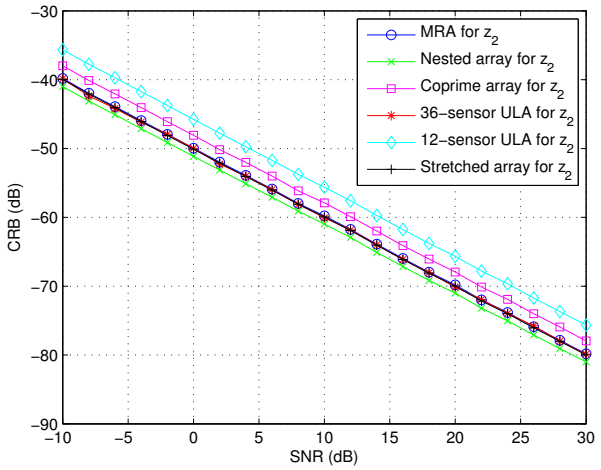

(b) CRBs for z_2

Figure 2. CRB comparisons with respect to per-sensor SNR, when the number of snapshots for all arrays set as $N = 720$, except for $N_{ula} = 200$, in the first-order measurement model.

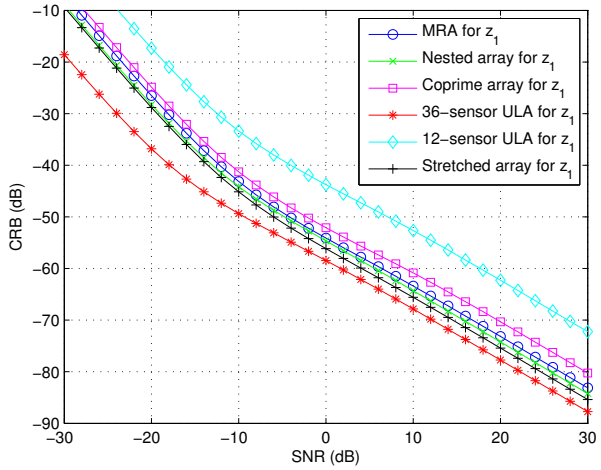

(a) CRBs for z_1

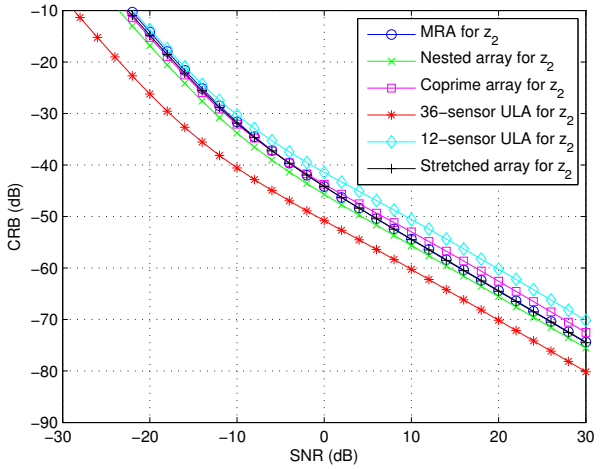

(b) CRBs for z_2

Figure 3. CRB comparisons with respect to per-sensor SNR, when the number of snapshots for all arrays set as $N = 200$ in the second-order measurement model.

Next, we increase the number of snapshots to $N = 1.2 \cdot \lceil 36/12 \rceil \cdot 200 = 720$ for all arrays, except for $\mathbb{I}_{ula}$, which still works with $N_{ula} = 200$ snapshots, and show the CRB results in Fig. 2. The improvements from Fig. 1 to Fig. 2 demonstrate that the CRB loss of SLAs in comparison with 36-sensor ULA due to smaller number of sensors can be compensated by larger number of snapshots, which is around the number of snapshots used by the 36-sensor ULA scaled by the compression ratio in the number of sensors.

4.2 CRB Comparisons in Second-Order Measurement Model

As in first-order measurement model, we continue to consider two modes, specified as $\boldsymbol{z} = [z_1, z_2]^T = [e^{j2\pi f_1}, 0.95 \cdot e^{j2\pi f_2}]^T$, with $f_1 = 0.14$ and $f_2 = 0.71$. The mode amplitude vectors are assumed to be i.i.d. drawn from $\mathcal{CN}[\mathbf{0}, \boldsymbol{\Sigma}]$, where $\boldsymbol{\Sigma} = \begin{bmatrix} 1 & \rho \\ \rho & 1 \end{bmatrix}$ with $\rho = 0.8$. In the second-order measurement model, the per-sensor SNR is

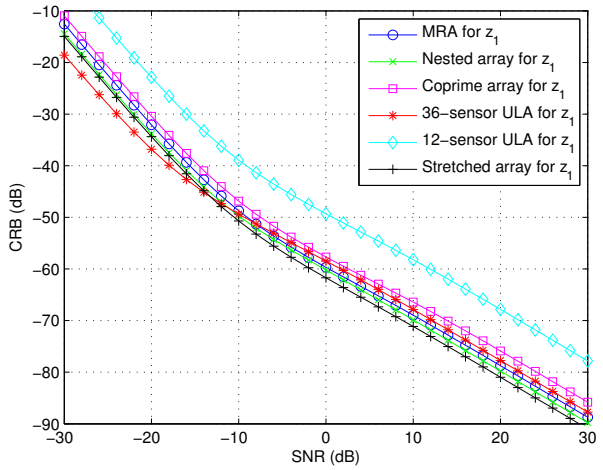

(a) CRBs for z_1

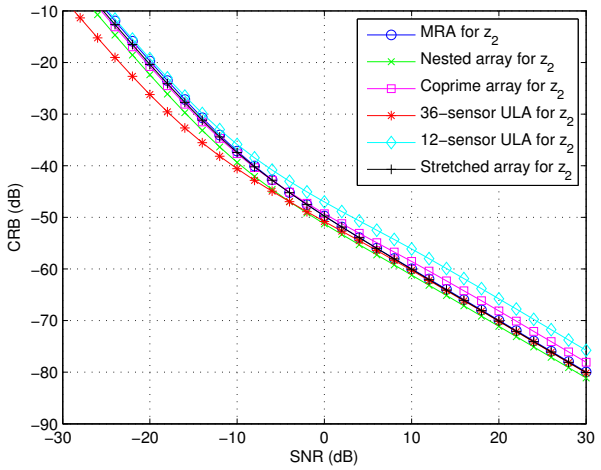

(b) CRBs for z_2

Figure 4. CRB comparisons with respect to per-sensor SNR, when the number of snapshots for all arrays set as $N = 720$, except for $N_{ula} = 200$, in the second-order measurement model.

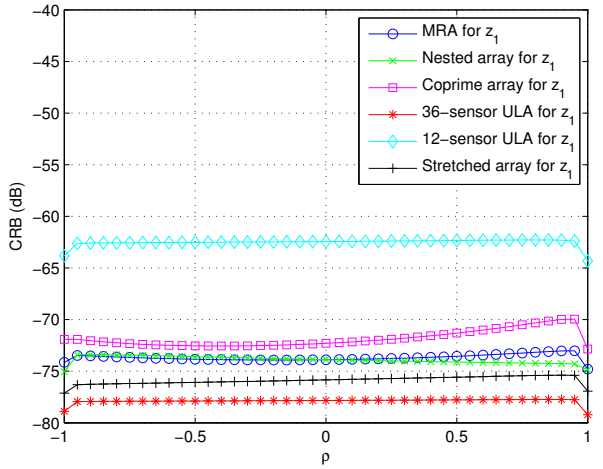

(a) CRBs for z_1

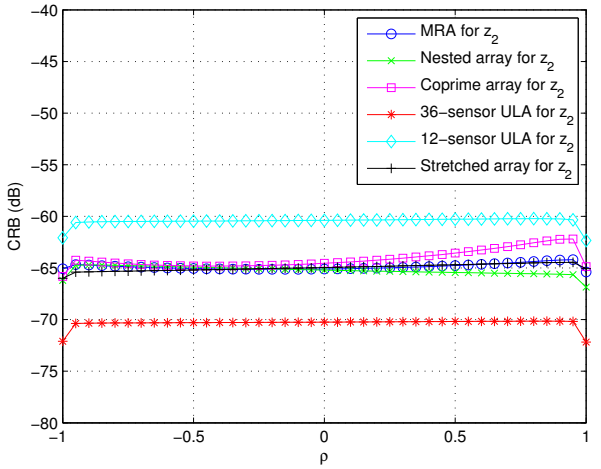

(b) CRBs for z_2

Figure 5. CRB comparisons with respect to correlation coefficient ρ, when the number of snapshots for all arrays set as $N = 200$ in the second-order measurement model.

defined as

$$\mathrm{SNR}_s\left(\boldsymbol{z},\mathbb{I}\right) = 10\log_{10}\frac{\mathbb{E}\left[\left\|\boldsymbol{V}\left(\boldsymbol{z},\mathbb{I}\right)\boldsymbol{x}\left[n\right]\right\|_2^2\right]}{m\sigma_e^2} = 10\log_{10}\frac{\mathrm{Tr}\left(\boldsymbol{V}\left(\boldsymbol{z},\mathbb{I}\right)\boldsymbol{\Sigma}\boldsymbol{V}^H\left(\boldsymbol{z},\mathbb{I}\right)\right)}{m\sigma_e^2}. \tag{17}$$

To simplify calculation, here we assume only the mode parameters $\boldsymbol{z}$ are the unknown variables. Setting the number of snapshots for all arrays as $N = 200$, we depict the CRB results of mode estimation with respect to per-sensor SNR in Fig. 3. Then increasing the number of snapshots to $N = 1.2 \cdot \lceil 36/12 \rceil \cdot 200 = 720$ for all arrays, except for $\mathbb{I}_{ula}$, which remains $N_{ula} = 200$, the CRB results are shown in Fig. 4. Note that a threshold phenomenon appears in the second-order measurement model. The CRB change trend is divided into two stages by the threshold, that is the CRB changes fast with respect to low per-sensor SNR, while exhibits a relatively slower change rate once the per-sensor SNR goes above the threshold. With large per-sensor SNR, the CRB compensation for SLAs brought by more snapshots is verified by the comparisons between Fig. 3 and Fig. 4.

Next, fixing the per-sensor SNR $\mathrm{SNR}_s\left(\boldsymbol{z},\mathbb{I}\right)$ to be 20 dB and keeping the mode setting, we examine the CRB

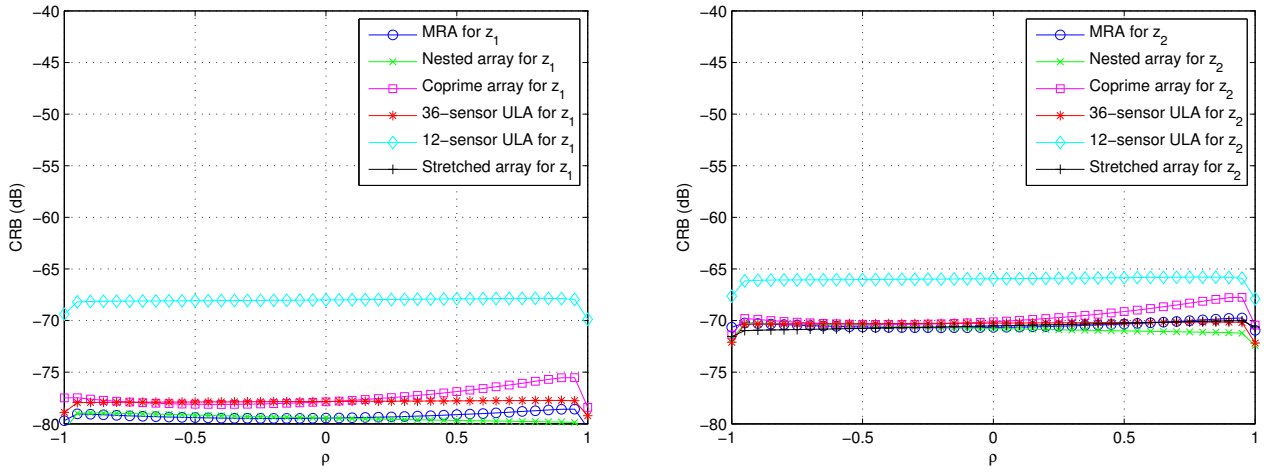

(a) CRBs for z_1 (b) CRBs for z_2

Figure 6. CRB comparisons with respect to correlation coefficient ρ, when the number of snapshots for all arrays set as $N = 720$, except for $N_{ula} = 200$, in the second-order measurement model.

compensation effect with respect to the correlation coefficient ρ in the covariance matrix $\mathbf{\Sigma}$ of mode amplitude generation. Similarly, we conduct two numerical experiments, one with $N = 200$ for all arrays, while the other one with $N = 1.2 \cdot \lceil 36/12 \rceil \cdot 200 = 720$ for all arrays, except for $N_{ula} = 200$. The CRB results with respect to correlation coefficient ρ are shown in Fig. 5 and Fig. 6, respectively. Both Fig. 5 and Fig. 6 imply that the change of correlation coefficient ρ has little impact on CRB, especially for ULAs, except for the points $\rho = \pm 1$. The CRB compensation of SLAs thanks to a larger number of snapshots can also be observed in Fig. 6.

These numerical results provide an evidence for that exploiting certain times as many snapshots as the 36-sensor ULA, which is about the compression ratio in the number of sensors adjusted by some constant, SLAs can achieve comparable CRB performance as the 36-sensor ULA in the second-order measurement model. In fact, recalling Eq. (7), we know that the CRB matrix $\mathbf{CRB}_s(\boldsymbol{\alpha}, \mathbb{I}_s)$ in second-order measurement model has a clear inversely proportional relationship with respect to the number of snapshots N, regardless of mode amplitude realization. However, the theoretical analysis about CRB comparison between two arrays will be more involved for the sake of complicated expression of $\mathbf{CRB}_s(\boldsymbol{\alpha}, \mathbb{I}_s)$ and is left for future work.

5. COMPARISONS OF MISSPECIFIED CRB

In this section, we carry out numerical experiments to investigate the behaviors of both ULA and SLAs under model misspecification, caused by sensor location perturbations.

Suppose only one undamped mode exists, denoted by $z_t = e^{j2\pi f_t}$ with $f_t \in [0, 1)$, and a linear array is composed of m_s sensors, nominally specified as $\mathbb{I}_s = \{i_0, i_1, \ldots, i_{m_s-1}\}$. In practice, usually the sensors can not be installed precisely, which will introduce position errors. Denote the position error imposed on the i_kth sensor by ϵ_k, $k = 0, 1, \ldots, m_s - 1$, and assume ϵ_k's are i.i.d. generated from a uniform distribution $\mathcal{U}[-0.2, 0.2]$. Then the true distribution for the measurement data can be represented as

$$g(\boldsymbol{y}) = \mathcal{CN}(\boldsymbol{d}, \boldsymbol{I}), \tag{18}$$

where $\boldsymbol{d} = s_t \cdot \left[e^{j2\pi f_t(i_0+\epsilon_0)}, e^{j2\pi f_t(i_1+\epsilon_1)}, \ldots, e^{j2\pi f_t(i_{m_s-1}+\epsilon_{m_s-1})}\right]^T \in \mathbb{C}^{m_s}$, which is the true steering vector of the array, multiplied by the true complex amplitude s_t. The true noise covariance, denoted by $\boldsymbol{I}$, is an identity matrix.

On the other hand, the user assumes a different distribution for the measurement data, expressed as

$$f(\boldsymbol{y}) = \mathcal{CN}(\boldsymbol{r}, \boldsymbol{R}), \tag{19}$$

where $\boldsymbol{r} = s \cdot \boldsymbol{v}$, of which $\boldsymbol{v}$ is the steering vector without taking the position errors into account, defined as $\boldsymbol{v} = [e^{j2\pi f i_0}, e^{j2\pi f i_1}, \ldots, e^{j2\pi f i_{m_s-1}}]^T \in \mathbb{C}^{m_s}$. The assumed noise covariance is set to be known and same as the true one as $\boldsymbol{R} = \boldsymbol{I}$.

For each numerical experiment in this section, only one measurement snapshot is available. The unknown parameters are f and s, and the corresponding ground truth is f_t and s_t, respectively. While treating s_t as a nuisance complex parameter, for the estimators of f_t, whose mean and estimator-score function correlation matrix are imposed the same constraints with maximum-likelihood, the MCRB with single snapshot can be obtained from the results in Ref. 14.

The array configurations explored here are same with those in Sec. 4. The comparisons of usual CRBs and the MCRB confidence intervals are shown in Fig. 7, with respect to per-sensor SNR, where each MCRB confidence interval, indicated by a pair of upper bound (U) and lower bound (L), is obtained from multiple realizations of the position errors. It seems the distances between usual CRBs and MCRBs are independent on the per-sensor SNR. $\mathbb{I}_{ula}$ has the smallest MCRBs, while $\mathbb{I}_{ula-short}$ has the largest MCRBs. Besides, $\mathbb{I}_{stretched}$ has the smallest MCRBs among all the 12-sensor arrays. Since $\mathbb{I}_{mra}$, $\mathbb{I}_{nested}$ and $\mathbb{I}_{coprime}$ have comparable performance, only the MCRBs of $\mathbb{I}_{coprime}$ are provided in Fig. 7 as a representative.

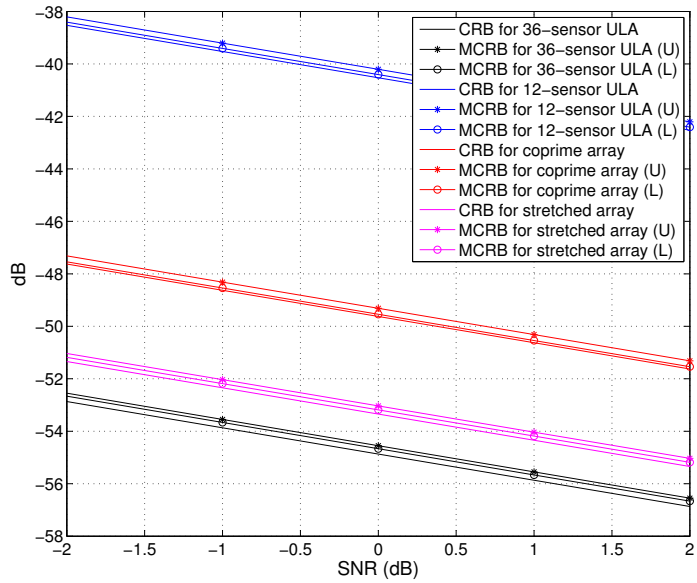

Figure 7. Comparisons of CRBs and the MCRB confidence intervals with respect to per-sensor SNR.

To see more details, fix the per-sensor SNR to be 0 dB, then the CRB and MCRB confidence interval of each array are shown in Fig. 8, where the blue marks represent the usual CRBs when no sensor perturbation is involved, and the red line segments represent the MCRB confidence intervals. Figure 8 (a) provides a comparison among all the arrays with a same y-axis, while in Fig. 8 (b), the comparisons are zoomed in. The SLAs not only yield a larger MCRB than the 36-sensor ULA on mode parameter estimation, but also bear wider MCRB confidence intervals.

6. CONCLUSION

In this paper, we investigate the CRB comparisons between a dense ULA and the embedded SLAs with the same aperture. Under the scenario of estimating one undamped mode, we theoretically show that SLAs can achieve comparable performance as ULA in terms of CRB, if the number of snapshots given for SLAs is about the number of snapshots used by ULA times the compression ratio in the number of sensors. This claim is further

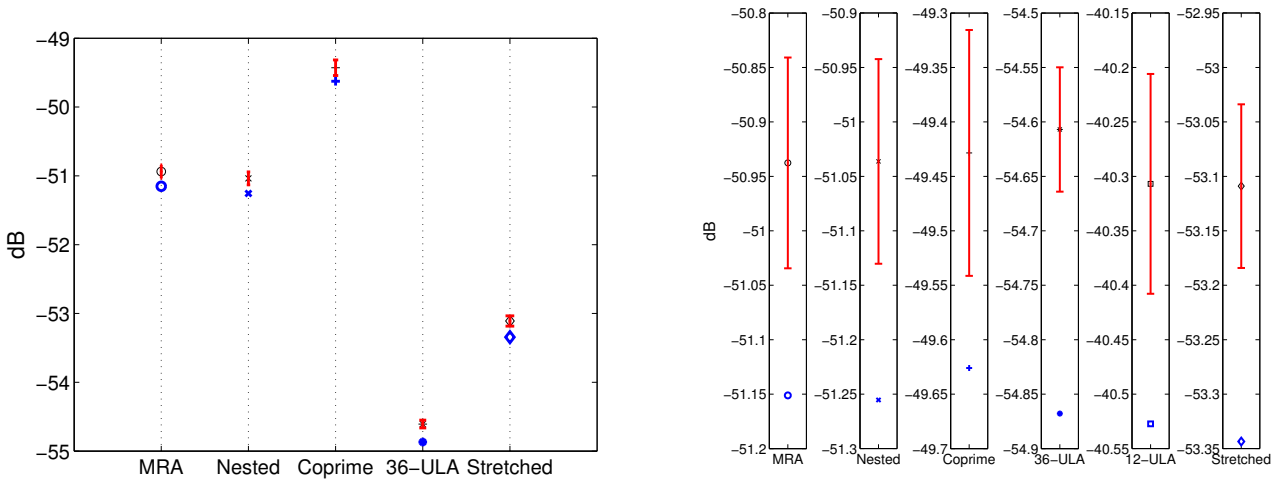

(a) (b)

Figure 8. Comparisons of CRBs and the MCRB confidence intervals, when the per-sensor SNR is 0 dB.

validated via numerical experiments in more complex scenarios. Moreover, the MCRBs of ULA and SLAs on mode parameter estimation are numerically compared under model misspecification. In the future, it will be of great interest to extend the theory in one undamped mode scenario to cases involved with multiple modes.

APPENDIX A. PROOF OF THEOREM 1

During this proof, we assume that m_s is an even integer satisfying $2 \leq m_s \leq m$. Similar argument works for an odd m_s as well.

For an arbitrary m_s-sensor array specified by $\mathbb{I}_s = \{i_0, i_1, \ldots, i_{m_s-1}\} \subseteq \mathbb{I}_{ula}$, we will show that the corresponding $J_f(z_1, \mathbb{I}_s)$ is not larger than $J_f(z_1, \mathbb{I}_{s-optimal})$, where $\mathbb{I}_{s-optimal} = \{0, 1, \ldots, m_s/2-1\} \cup \{m-m_s/2, m-m_s/2+1, \ldots, m-1\}$.

Without loss of generality, assume the elements in $\mathbb{I}_s$ are in ascending order, that is $i_0 < i_1 < \cdots < i_{m_s-1}$, then the proof idea is as follows. In the first stage, starting from $\mathbb{I}_s$, we move the first half sensors, i.e. $i_0, i_1, \ldots, i_{m_s/2-1}$, to the left most in the order of their indices. Specifically, via the lth move operation, the sensor i_{l-1} will be moved to the location $l-1$, for $1 \leq l \leq m_s/2$. Next, in the second stage, the left half sensors, i.e. $i_{m_2/2}, i_{m_2/2+1}, \ldots, i_{m_s-1}$, will be moved to the right most in the reverse order of their indices. To put it in other words, via the lth move operation, the sensor $i_{3m_s/2-l}$ will be moved to the location $m + m_s/2 - l$, for $m_s/2 + 1 \leq l \leq m_s$. Finally, $\mathbb{I}_s$ will be transformed into $\mathbb{I}_{s-optimal}$ via these move operations. Denote the array after lth move operation by $\mathbb{I}_{s_l}$, then the left work is to show that $J_f(z_1, \mathbb{I}_{s_l})$ is a non-decreasing function with respect to l.

Let's consider the first stage. After the first move operation, the array can be represented as $\mathbb{I}_{s_1} = \{0\} \cup \{i_1, i_2, \ldots, i_{m_s-1}\}$ and it is not difficult to verify $J_f(z_1, \mathbb{I}_{s_1}) \geq J_f(z_1, \mathbb{I}_s)$. For $1 \leq l \leq m_s/2 - 1$, after the lth move operation, the array is rearranged to be $\mathbb{I}_{s_l} = \{0, 1, \ldots, l-1\} \cup \{i_l, i_{l+1}, \ldots, i_{m_s-1}\}$. During the $l+1$th move operation, we will move i_l to the location l, and consequently obtain the array as $\mathbb{I}_{s_{l+1}} = \{0, 1, \ldots, l\} \cup \{i_{l+1}, i_{l+2}, \ldots, i_{m_s-1}\}$. Then we can calculate

$$\begin{aligned} m_s\left(J_f\left(z_1, \mathbb{I}_{s_{l+1}}\right) - J_f\left(z_1, \mathbb{I}_{s_l}\right)\right) &= \sum_{t=0}^{l-1}(l-t)^2 + \sum_{t=l+1}^{m_s-1}(l-i_t)^2 - \sum_{t=0}^{l-1}(i_l-t)^2 - \sum_{t=l+1}^{m_s-1}(i_l-i_t)^2 \\ &= \sum_{t=0}^{l-1}(l-t)^2 + \sum_{t=m_s-l}^{m_s-1}(l-i_t)^2 - \sum_{t=0}^{l-1}(i_l-t)^2 - \sum_{t=m_s-l}^{m_s-1}(i_l-i_t)^2 \end{aligned}$$

$$
\begin{aligned}
&+\sum_{t=l+1}^{m_s-l-1}\left[(l-i_t)^2-(i_l-i_t)^2\right] \\
&\geq \sum_{t=0}^{l-1}(l-t)^2+\sum_{t=m_s-l}^{m_s-1}(l-i_t)^2-\sum_{t=0}^{l-1}(i_l-t)^2-\sum_{t=m_s-l}^{m_s-1}(i_l-i_t)^2 \qquad (20)\\
&=\sum_{t=0}^{l-1}\left[(l-t)^2+(l-i_{m_s-1-t})^2-(i_l-t)^2-(i_l-i_{m_s-1-t})^2\right] \\
&=2\sum_{t=0}^{l-1}(i_l-l)\left(t+i_{m_s-1-t}-l-i_l\right) \\
&\geq 0, \qquad (21)
\end{aligned}
$$

where the inequality Eq. (20) comes from the fact that $l \leq i_l < i_t$, for $t \geq l+1$, and the inequality Eq. (21) comes from the fact that for $1 \leq l \leq m_s/2-1$ and $t < l$, there is $i_{m_s-1-t} - i_l \geq i_{m_s-1-t} - i_{m_s-1-l} \geq (m_s-1-t)-(m_s-1-l) = l-t$. Therefore, we have $J_f\left(z_1, \mathbb{I}_{s_{l+1}}\right) - J_f\left(z_1, \mathbb{I}_{s_l}\right) \geq 0$, for $1 \leq l \leq m_s/2-1$.

Next, employing the similar proof techniques, we can also show that $J_f\left(z_1, \mathbb{I}_{s_l}\right)$ is a non-decreasing function with respect to l in the second stage. This completes the proof.

APPENDIX B. PROOF OF THEOREM 2

According to the configurations of $\mathbb{I}_{ula}$ and $\mathbb{I}_{s-optimal}$, we can calculate Eq. (10) for each array as

$$
J_f\left(z_1, \mathbb{I}_{ula}\right) = \frac{1}{12} m\left(m^2-1\right), \quad \text{and} \quad J_f\left(z_1, \mathbb{I}_{s-optimal}\right) = \frac{1}{12} m_s\left(m_s^2 - 3mm_s + 3m^2 - 1\right),
$$

respectively. Then we get

$$
\frac{J_f\left(z_1, \mathbb{I}_{ula}\right)}{J_f\left(z_1, \mathbb{I}_{s-optimal}\right)} = \frac{m\left(m^2-1\right)}{m_s\left(m_s^2 - 3mm_s + 3m^2 - 1\right)} \leq \eta \cdot \frac{m^2-1}{m^2-1} = \eta,
$$

and

$$
\frac{J_f\left(z_1, \mathbb{I}_{ula}\right)}{J_f\left(z_1, \mathbb{I}_{s-optimal}\right)} = \frac{m\left(m^2-1\right)}{m_s\left(m_s^2 - 3mm_s + 3m^2 - 1\right)} \geq \eta \cdot \frac{m^2-1}{3\left(m-1\right)^2} \geq \frac{1}{3}\eta,
$$

when $2 \leq m_s \leq m$.

ACKNOWLEDGMENTS

This material is based upon work supported in part by the Air Force Office of Scientific Research under award number FA9550-15-1-0205, and by the Office of Naval Research under award number N00014-15-1-2387.

REFERENCES

[1] Moffet, A., "Minimum-redundancy linear arrays," *IEEE Transactions on antennas and propagation* **16**(2), 172–175 (1968).

[2] Pal, P. and Vaidyanathan, P., "Nested arrays: A novel approach to array processing with enhanced degrees of freedom," *IEEE Transactions on Signal Processing* **58**(8), 4167–4181 (2010).

[3] Vaidyanathan, P. P. and Pal, P., "Sparse sensing with co-prime samplers and arrays," *IEEE Transactions on Signal Processing* **59**(2), 573–586 (2011).

[4] Pal, P. and Vaidyanathan, P. P., "Coprime sampling and the music algorithm," in [*Digital Signal Processing Workshop and IEEE Signal Processing Education Workshop (DSP/SPE), 2011 IEEE*], 289–294, IEEE (2011).

[5] Vaidyanathan, P. and Pal, P., "Direct-music on sparse arrays," in [*Signal Processing and Communications (SPCOM), 2012 International Conference on*], 1–5, IEEE (2012).

[6] Vaidyanathan, P. and Pal, P., "Why does direct-music on sparse-arrays work?," in [*Signals, Systems and Computers, 2013 Asilomar Conference on*], 2007–2011, IEEE (2013).

[7] Pakrooh, P., Scharf, L. L., and Pezeshki, A., "Modal analysis using co-prime arrays," *IEEE Transactions on Signal Processing* **64**(9), 2429–2442 (2016).

[8] Stoica, P. and Nehorai, A., "Music, maximum likelihood, and cramer-rao bound," *IEEE Transactions on Acoustics, Speech, and Signal Processing* **37**(5), 720–741 (1989).

[9] Stoica, P. and Nehorai, A., "Performance study of conditional and unconditional direction-of-arrival estimation," *IEEE Transactions on Acoustics, Speech, and Signal Processing* **38**(10), 1783–1795 (1990).

[10] Wang, M. and Nehorai, A., "Coarrays, music, and the cramér–rao bound," *IEEE Transactions on Signal Processing* **65**(4), 933–946 (2016).

[11] Koochakzadeh, A. and Pal, P., "Cramér–rao bounds for underdetermined source localization," *IEEE Signal Processing Letters* **23**(7), 919–923 (2016).

[12] Liu, C.-L. and Vaidyanathan, P., "Cramér–rao bounds for coprime and other sparse arrays, which find more sources than sensors," *Digital Signal Processing* **61**, 43–61 (2017).

[13] Li, Y. and Chi, Y., "Off-the-grid line spectrum denoising and estimation with multiple measurement vectors," *IEEE Transactions on Signal Processing* **64**(5), 1257–1269 (2016).

[14] Richmond, C. D. and Horowitz, L. L., "Parameter bounds on estimation accuracy under model misspecification," *IEEE Transactions on Signal Processing* **63**(9), 2263–2278 (2015).

[15] Schreier, P. J. and Scharf, L. L., [*Statistical signal processing of complex-valued data: the theory of improper and noncircular signals*], Cambridge University Press (2010).